

Study and optimization of RPCs for high rate applications

*P. Carlson¹, I. Crotty², P. Cwetanski^{2,3}, T. Francke¹, P.Fonte⁴,
V. Peskov¹ and A. Sharma^{2*}*

¹Royal Institute of Technology, Stockholm, Sweden

²CERN, CH 1211 Geneva, Switzerland

³Helsinki Institute of Physics, Helsinki, Finland

⁴ISEC and LIP, Coimbra, Portugal

Abstract

Due to the low cost, good time resolution and the properties of RPCs with respect to electronics damage protection, they are chosen for many large experiments. These detectors are reliable and stable in their operation with counting rates up to kHz/cm². The aim of this work is to understand the fundamental rate limits of RPCs in order to find an efficient way for their optimization and hence, extend their applications. Several types of materials have been used and operational parameters have been optimized in this work comprising simulations and experiment. High efficiency, excellent position resolution, low noise and high rate capability is demonstrated. These type of RPCs open new avenues in several applications, for example in crystallography, biology and medicine.

Paper presented at the Nuclear Science Symposium and Medical Imaging Conference, San Diego, USA Nov 4-10, 2001

* Corresponding author

A. Sharma CERN, CH 1211, Geneva Switzerland Archana.Sharma@cern.ch

Tel: + 41 22 767 8969, GSM: +41 79 201 4875, Fax: + 41 22 767 9070

I. Introduction

Due to the low cost, good time resolution and electronics damage protection properties Resistive Plate Chambers, (RPCs) are chosen for many large scale experiments for LHC at CERN and in other experiments elsewhere, for example: ATLAS, CMS, ALICE and MONOLITH. These detectors are reliable and stable in their operation with counting rates of 100-1000 Hz/cm². At higher rates RPCs made of conventional materials (melamine, phenolic, glass) suffer from charging up effects, excessive current and an unacceptable high rate of noise (spurious) pulses, both in avalanche and streamer mode of operation. The first successful attempts to develop RPCs made of new low resistivity materials capable of operating at even higher rates were described in ref. [1,2]. In this work we have performed the optimization of this promising type of RPC. The ultimate goal was to build and test extremely high rate RPCs for biological and medical applications. The work was performed in two parallel directions: simulation and experimental work. Simulations have allowed us to better understand the electrostatic field configuration, as well as perform geometry optimizations. The experimental part of the work permitted a verification and final tuning of RPCs. Below we present the progress in the developments of position-sensitive high-rate RPCs.

II. Experimental set up

Our experimental set up (see Fig.1) consists of an aluminium gas chamber inside which various designs of RPCs (sizes 5x5cm² and 10x10cm²) could be installed and tested: for example, designs without spacers between electrodes or with spacers of various geometry, see table 1. The gap between electrodes could be varied from 0.1 to a few mm. Some designs of RPCs had metallic readout strips of 50 μ m or 350 μ m pitch on the inner or outer parts of electrodes allowing a performance of high accuracy position measurements.

| <i>Material</i> | <i>Resistivity ($\Omega.cm$)</i> | <i>Gap/ Spacer thickness (mm)</i> | <i>Gas</i> | <i>Thickness / Coating</i> |
|---------------------------|---|---|------------|--------------------------------|
| Pestov Glass | $10^{10}-10^{12}$ | 0.1-3mm | All | 2-5 mm |
| n- and p-type Silicon | $0.1 - 2.10^4$ | 0.1 - 1 | All | 0.5 - 2 mm |
| Ceramics | 10^9-10^{11} | 0.4 - 1 | All | 2-3 |
| Ink-Based Epoxy | 10^7-10^{12} | | Ar based | |
| Phenolic | $5.10^8 - 3.10^{10}$ | 2-3 | | 2 mm |
| Bakelite | $10^{10}-10^{11}$ | 2-3 | Ar based | |
| Melamine | $10^{11} - 10^{12}$ | 1-2 | Ar based | CsI, 0.8 |
| Float Glass | $7.0.10^{12}$ | 2-3 | Ar based | 1.85 |
| Metallic | 0 | 1-3 | All | CsI, 5mm |
| “Welding” Schott Glass | $1.5.10^{12}$ | 0.1-2 | All | CsI, 3mm |

Table 1

Before assembling the glass, Si or ceramic based electrodes, they were ultrasonically cleaned in distilled soap water to remove any dust particles. The test chamber was

also carefully cleaned in the same way. RPCs with cathodes coated with uniform (0.3 μm thick) or porous CsI (up to 10 μm thick) layers as secondary electron emitters, see for example refs. [3-5] for more details, were also investigated.

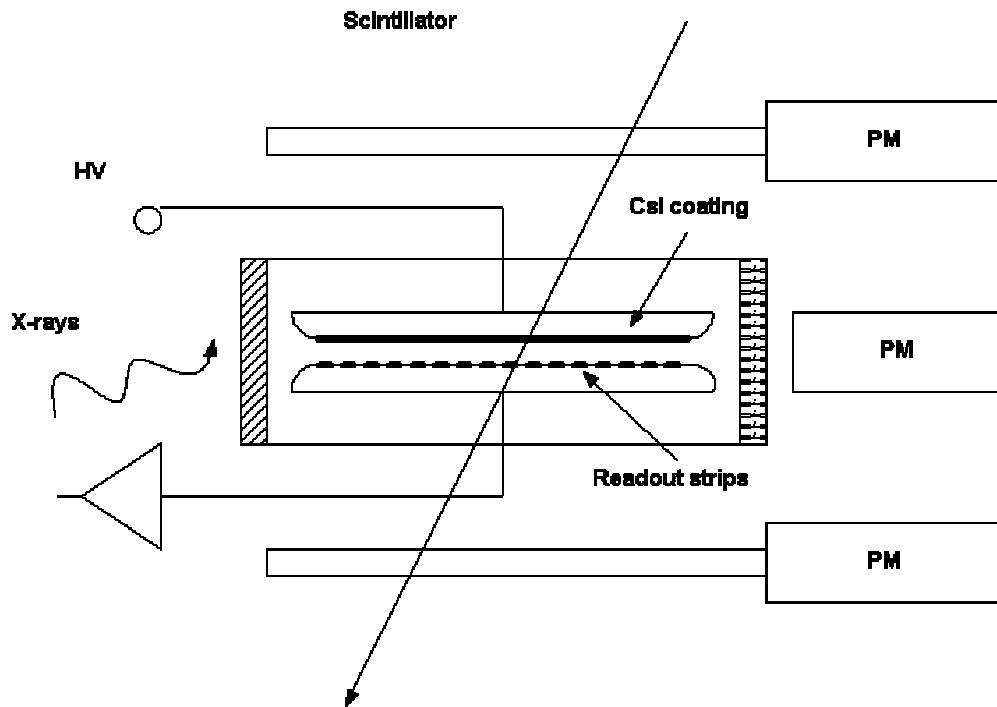


Fig. 1

For a comparison, “conventional” designs of RPCs made of phenolic/bakelite or melamine sheets were also studied. Typically their electrodes had a disc shape with a diameter of 70-80 mm and gaps between electrodes of 1-3mm.

All RPCs mentioned above were assembled in a clean room¹.

In addition, we have tested RPCs of large sizes: $1 \times 0.3 \text{m}^2$ and $0.25 \times 0.25 \text{m}^2$. made of glass (see table 1). They had their own gas [6,7] with metallic readout strips on the outside. Some cross check measurements were made with metallic parallel plate chambers with disc electrodes, 5 cm in diameter, made of stainless steel or copper. The spacers were placed outside the active area, ~ 2 cm offset from the edge, of the detector and the electrode edges were rounded.

Tests were performed in various gas mixtures containing Isobutane, Argon and Freon (R134a) as well as Argon/Ethane, and Argon or Xenon and Krypton mixtures with various quenchers and their combinations: CO_2 , ethane, alcohol and Freon. The percentages of each component were widely varied.

The ionization was caused by X-rays from an X-ray gun of 6-30 keV, betas ^{90}Sr and ^{106}Ru , gammas ^{60}Co , and by UV from a mercury lamp (in order to create single electrons). For measurements of the sizes of dead zones around spacers a lead sheet with a hole of $\text{\O} 100 \mu\text{m}$ was used. The lead sheet was placed in contact with the cathode plane and moved perpendicular to the readout strips. For position resolution measurements with X-rays a slit $30 \mu\text{m}$ wide, oriented perpendicular to the electrode

¹ Class 1000

plane was used. The slit could be moved in the direction perpendicular to the strips with an accuracy of a few μm , the efficiency of detection of minimum ionizing particles could be measured using cosmic muons. They were identified by coincidence of signals from two scintillators (see Fig.1). In an avalanche mode of operation, signals from the RPCs were measured at low rates with charge sensitive amplifiers, and at high rates with current amplifiers. In the streamer mode operation, signals were directly monitored on two beams storage LeCroy scopes. In addition in some measurements we used a PM to detect the light produced by avalanches and streamers or visual observations. For leakage current measurements a Kiethley picoamperometer was used.

III. Results

III-1. Optimization of Geometry, Materials and Gas mixture

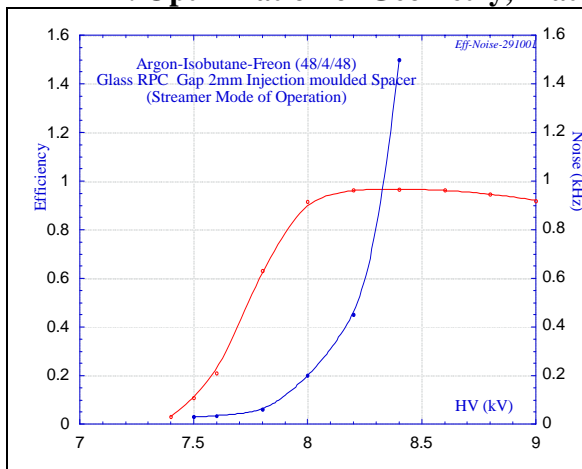


Fig. 2 (a)

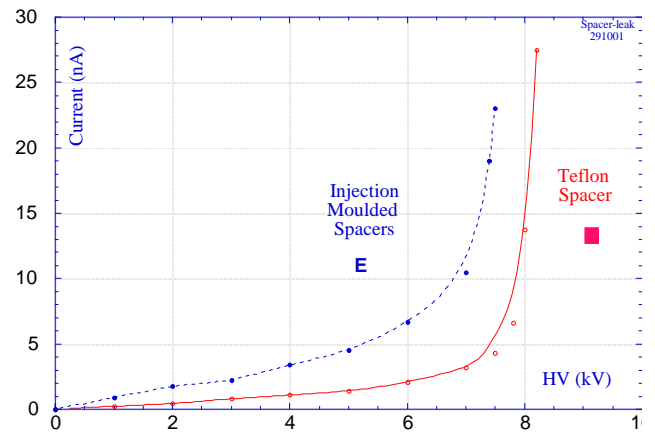


Fig. 2(b)

As was mentioned before, at counting rates greater than 10^3 Hz/cm^2 RPCs manufactured with conventional materials (melamine, glass, bakelite) suffer from several problems: charging up effect, leakage current, noise. As was demonstrated in our earlier works [2], the charging up effect can be strongly diminished by using low resistivity materials for the electrodes. In this case RPC combine high rate capability, almost approaching the limits of a metallic parallel plate chamber [2]), and maintaining the desirable spark protective property. However the remaining problems: high leakage current and noise need to be solved, hence it is very important to understand the origin of the leakage current and noise pulses. It is natural to assume that the leakage current consists of two components, a leakage through spacers and a current due to the noise. As a first step we focus our studies on the optimization of spacers. Fig. 2a shows the typical dependence of the leakage current, noise pulses rate and efficiency vs. the applied voltage in an RPC. One can see that at relatively low voltages the leakage current increases almost linearly and at higher voltage starts growing almost exponentially.

One can assume that the linear part is due to the leakage current through spacers whereas the “exponential” part is due to noise pulses. To verify this assumption prototypes of RPCs were built with spacers placed far away from the amplification gap with a specialized (see later) dielectric spacer. Indeed the linear part of the current decreased almost an order of magnitude. The material of the spacer is equally

important as seen in Fig. 2(b). A careful design of the spacers and edges may reduce one of the component of the leakage current. The optimization of spacers and edges was performed in two steps, simulations studies and experimental verification before the final tuning.

a) Simulation

The RPC model represents only a reduced cell of symmetry (Fig. 3) for the finite element computation comprising the Bakelite electrodes with a frame and spacers that form the gas gap. A 100 μm thick graphite coating was applied on top of the Bakelite to define the HV source. Although the operation of an RPC should be described with models involving surface and volume currents an electrostatic approach can be justified under the condition of small overall currents (low particle rate) and sufficiently low resistivity. Nevertheless qualitative conclusions may be drawn. Detailed analytic calculations of the electric field in RPCs involving current flow can be found in [9].



Figure 3: Model of a reduced cell of symmetry.

- The electric field close to frame and spacers

An advantageous effect of dielectric spacers in the active region can be the bundling of field lines inside the dielectric, weakening the field around the spacer (Fig. 4), which however is not valid for all geometries. Furthermore spacers are like the frame a conductive contribution to the overall leakage current in the chamber. Therefore a careful design is indispensable for reliable operation. Although the frame shape has an influence on the leakage current, from an electrostatic point of view it should not be a region of local discharges, since the graphite coating is offset by 20 – 25 mm with respect to the inner frame wall. Thus the electric field in the gas gap close to the frame is far below amplification threshold.



Figure 4: Electric field in the gas gap around a cylindrical Polycarbonate button.

- Spacer buttons

The effect of field bundling for a cylindrical spacer (Polycarbonate) can be seen in the following plot. The absolute field values may not correspond to operating conditions, they are rather a qualitative indicator.

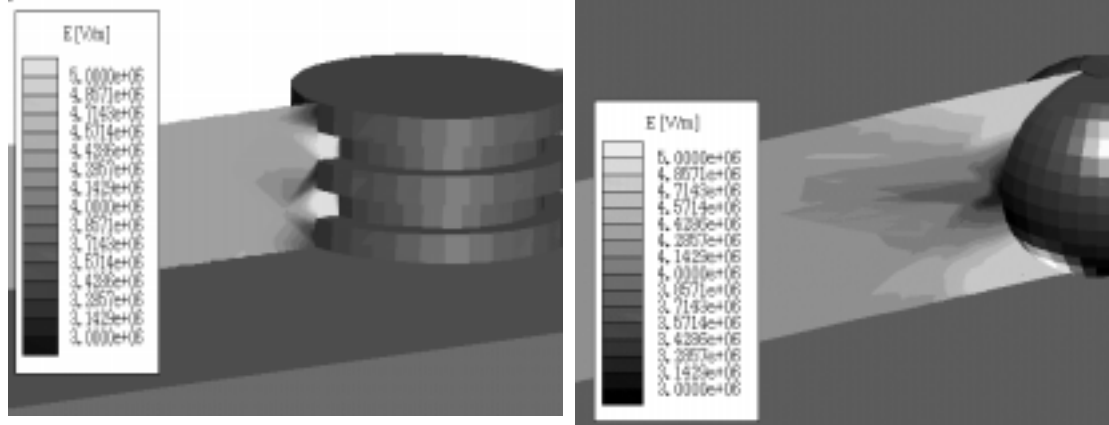


Fig. 5 (a,b): Electric field in the gas gap around an E-shaped and spherical spacer.

- Frame edges

As mentioned before the choice of the frame cross-section geometry is based on the desire to minimize leakage currents. In Figures 6 (a,b) electric field flux lines are drawn for two different frame cross-sections. From an electrostatic point of view the square-shaped frame would be favorable. However the T-shaped frame increases the surface resistivity and hence leakage current is reduced. This is actually observed in the measurements presented in the next section.

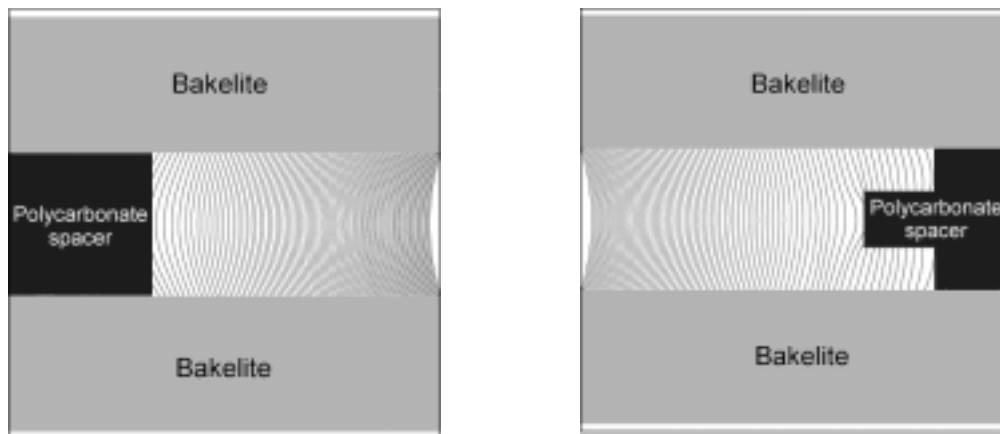


Figure 6 (a,b): Electric field flux lines close to a square-shaped and T-shaped frame

- Linseed drop or inclusion on the Bakelite surface

Linseed oil has been routinely applied to RPCs [10] to reduce resistivity and smoothen the surface. During the operation of the RPC, even small drops of linseed oil on the electrodes affect the homogeneity of the parallel plate field in the avalanche gap. The same is true for inclusions coming from dust particles, or any other pollution as modeled in fig. 7(a).

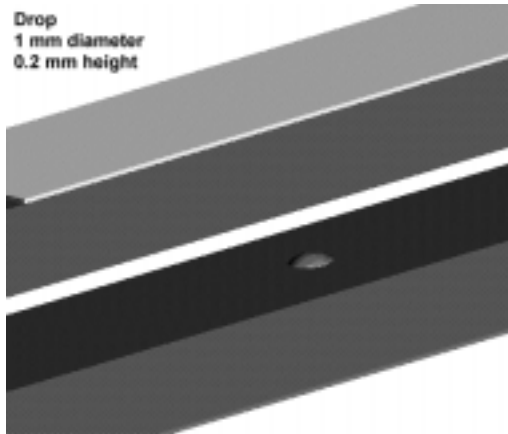


Fig. 7(a): Model of a 2 mm gap RPC with a droplet.

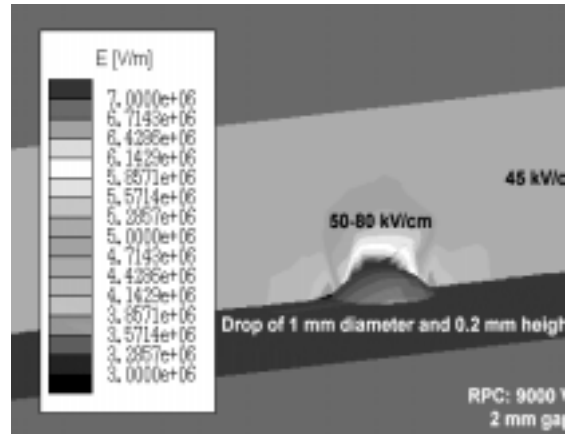


Fig. 7(b): Electric field distortion close to the droplet

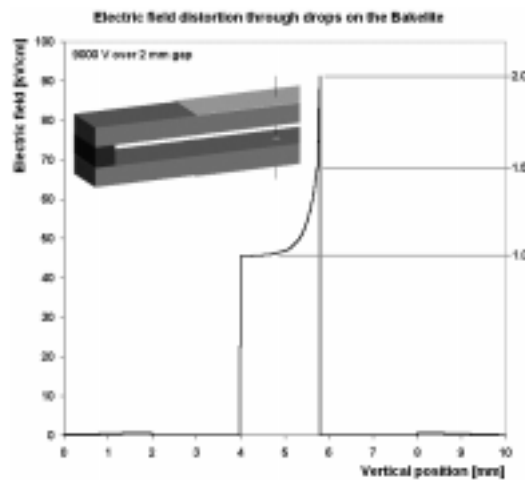


Figure 7(c): Field along a vertical line over the droplet.

We can see a clear enhancement of the electric field close to droplets due to a local gap width reduction (Fig. 7 b and c). This will possibly increase the streamer rate for chambers intended to work in avalanche mode. The droplet density plays here the crucial role.

- **Distance of the graphite coating from the edge**

A way to decrease chamber noise due to leakage currents and spurious pulses was found with increasing the offset of the graphite coating from the chamber edge. In the simulation we see that this leads to an exponential drop of the electric field in the gas gap at the edges as shown in the following line and 2-dimensional plots (Figs. 8 and 9). The experimental observation that an increase from 15 mm to 25 mm severely decreases noise by a factor of three [11] does not clearly follow from the electrostatic simulation. What becomes clear is that the electric field drops below amplification level ($\sim 30\text{--}35$ kV/cm in the common freon-based mixtures) already a few millimeters after the graphite coating edge.

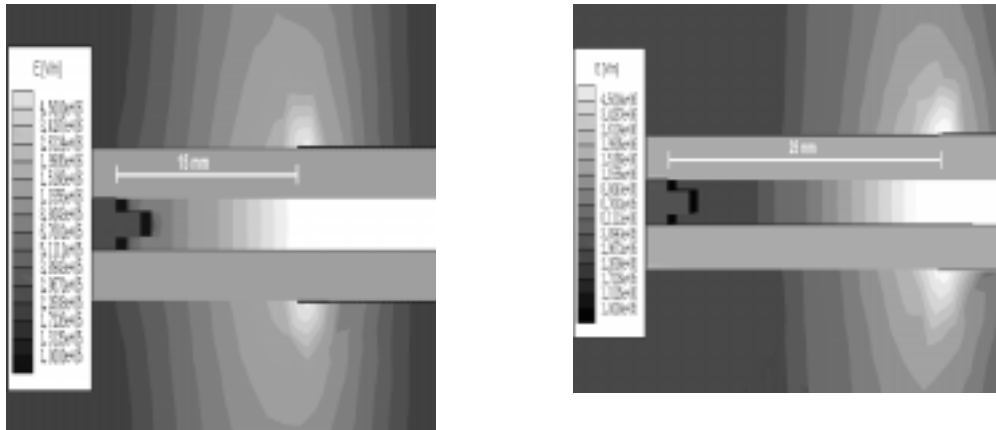


Fig. 8 (a,b): Electric field in the gas gap for various distances of the graphite coating from the inner frame wall

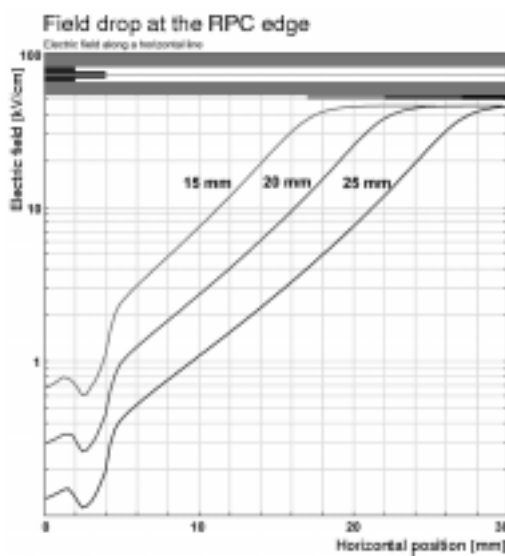


Figure 9a: Field along a horizontal line through the gas gap.

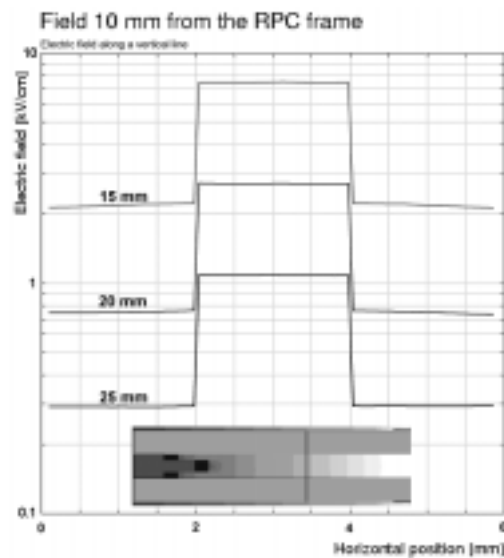


Figure 9b: Field along a vertical line 10 mm away from the frame edge.

- Gain, charge and efficiency vs. gas mixture

Reliable computation of electron avalanches is difficult due to lack of accuracy in the electron impact cross-sections of Tetrafluoroethane (TFE or $C_2H_2F_4$). Measurements of drift velocity and effective Townsend coefficient have been done by Gorini et al, but in a very narrow E/p range [12]. The measured behavior of the electron drift velocity computation seems questionable, making it difficult to extract cross-sections with acceptable accuracy [13]. The following plots (Fig. 10 a and b) show the simulated and measured drift velocities and Townsend as well as attachment coefficients for various freon-based gas mixtures.

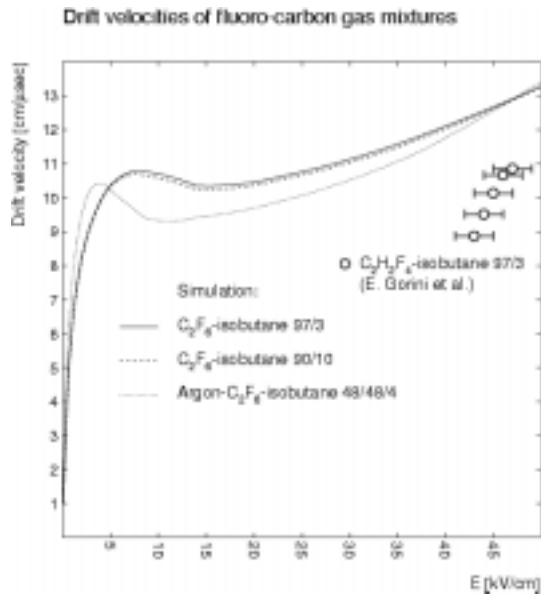


Fig.10a): Electron drift velocities for various freon-based mixtures.

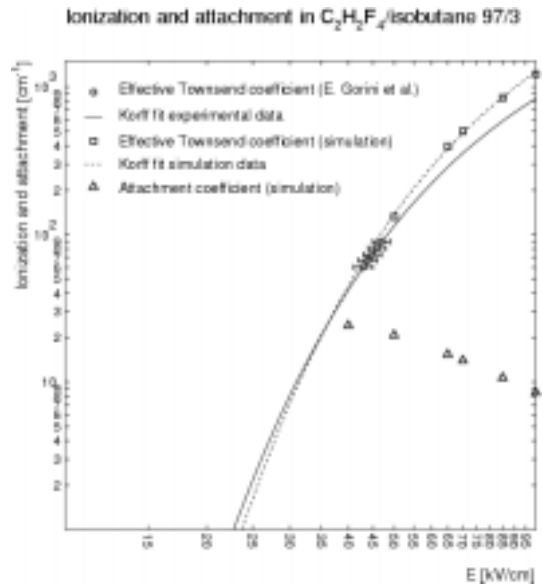


Fig. 10(b): Ionization coefficients for various freon-based mixtures.

However using the existing cross-sections with a simple avalanching model already leads to acceptable results (Fig. 11a). This might be a hint that in this electric field region the saturating effects in the avalanche still play a minor role. For electro-negative gas mixtures ionization and attachment are related to the chamber efficiency.

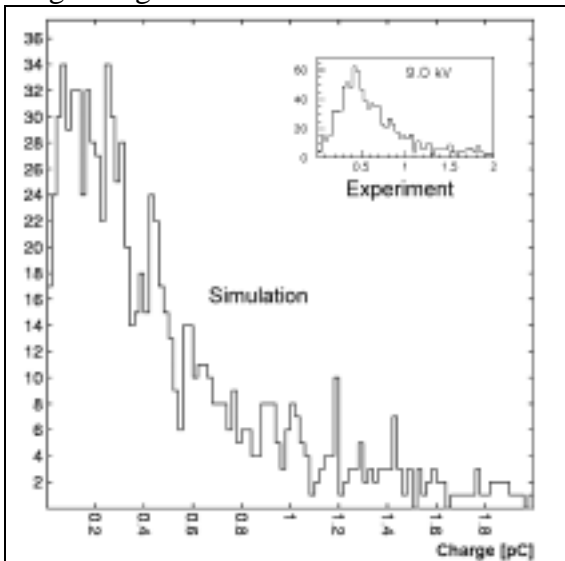


Fig.19: Simulated and measured charge spectrum.

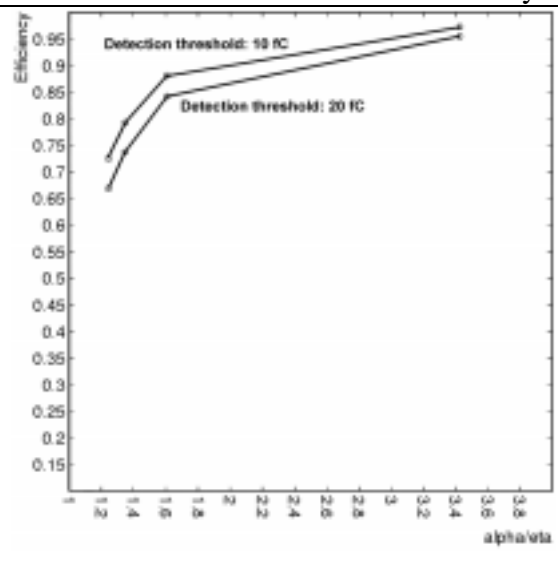


Fig.20: Simulated chamber efficiencies vs. ionization-attachment ratio.

Gorini et al have measured an effective Townsend coefficient (ionization minus attachment), which prevents an exact separation of the single coefficients. However large attachment values would not permit avalanches with a measurable overall charge due to large primary electron losses. A simulation indicates that a reasonable ionization-to- attachment ratio should be greater than three (Fig. 19 b). Still only careful measurements can lead to an accurate determination of the ionization parameters respectively electron impact cross-sections needed in detector simulations. Moreover an advanced model is needed to compute avalanche processes under dynamic electric field conditions considering the influence of space charges. An independent treatment of attachment and Townsend coefficient in the avalanche

computation is preferable for electro-negative gases [14]. W. Riegler et al have developed a simulation considering these effects, they however operate in perfectly parallel field geometries and therefore exclude studies of field distortions [15].

b) Experimental verification

- RPCs with amplification gap width 1-3 mm

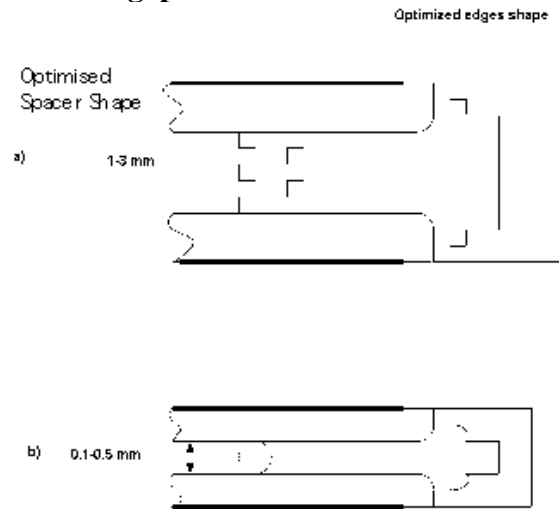


Fig. 12 (a,b)

Based on simulations we have optimized the spacers shape in such a way that there are regions on their surface parallel to the RPCs electrodes: grooves or cylindrical extensions (leakage current protective structures)-see Fig.12. Such spacers allow minimizing the surface leakage current, especially if the protective structure is large enough and prevents surface streamer development [8]. However a large protective structure gives a rather large dead zone (see Fig. 13).

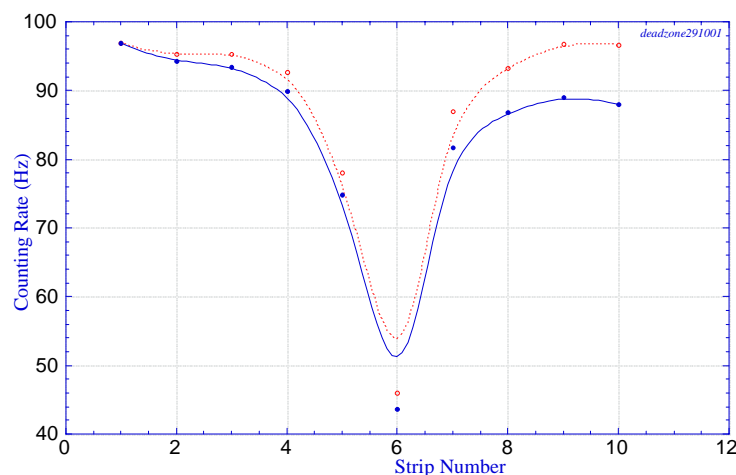


Fig. 13 Counting rates from strips ($350\mu\text{m}$ pitch) measured with the scanned hole. Melamine RPC, gap 3mm, dashed line - cylindrical, solid line - E-shaped.

The spacers should be made with a material of high volume and surface resistivity, for example Lexan, Noryl or Teflon. One should note however that at high rate, even operating with relatively low gains ($\sim 10^5$) these optimized spacers may create a problem: charging up the entire RPC electrodes due to absence of leakage current. This can be observed from Fig.2 (a,b): with Teflon spacers the leakage current was more, while for the same voltage the amplification was less due to the charging up of the electrodes. Therefore, it is extremely important to use low resistivity materials for electrodes even at moderate rates ($\sim 10^4 \text{ Hz/cm}^2$). In this case the leakage current through the electrode volume ensures a stable operation of the RPC (see Fig. 14).

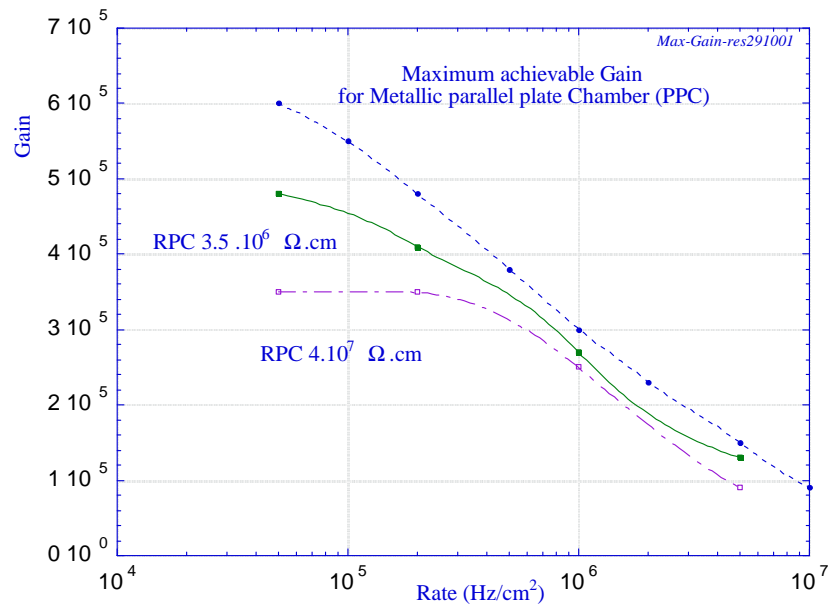


Fig. 14

- RPCs with small amplification gaps

Recently there has been a great interest in small gap RPCs due to their extremely good time resolution (better than 100 ps) [16]. It is technically difficult to manufacture spacers with protective structures at RPCs gap width 0.1-0.5mm. Thus one can only rely on good materials and on simple geometrical configurations. At low rate, cylindrical or ball shaped spacers made of quartz yield good results. However, at high rates, especially in the case of x-rays, breakdowns still may occur across the spacer surface, probably due to the radiation induced surface conductivity.

The main conclusion from these experimental studies is that one can optimize spacers, but for high rates they should be installed outside the active area of the RPC. The optimized shape of the edge interface is shown in (Fig. 21b); this result is not supported by the electrostatic simulations.

- Noise pulses

The “exponential “ part of the current is associated with noise pulses (see Fig.2). It was found that for all RPCs investigated, the rate of the noise pulses increases sharply when their efficiency to minimum ionizing particles reaches a plateau. Comparing their pulse-height spectra with those produced by UV photons, one can conclude that noise pulses are triggered not by single electrons, but by several primary electrons

emitted simultaneously from the cathode surface. By analyzing signals from the readout strips we concluded that most of the noise pulses are originating from the same fixed spots on the cathode surface (Fig. 15).

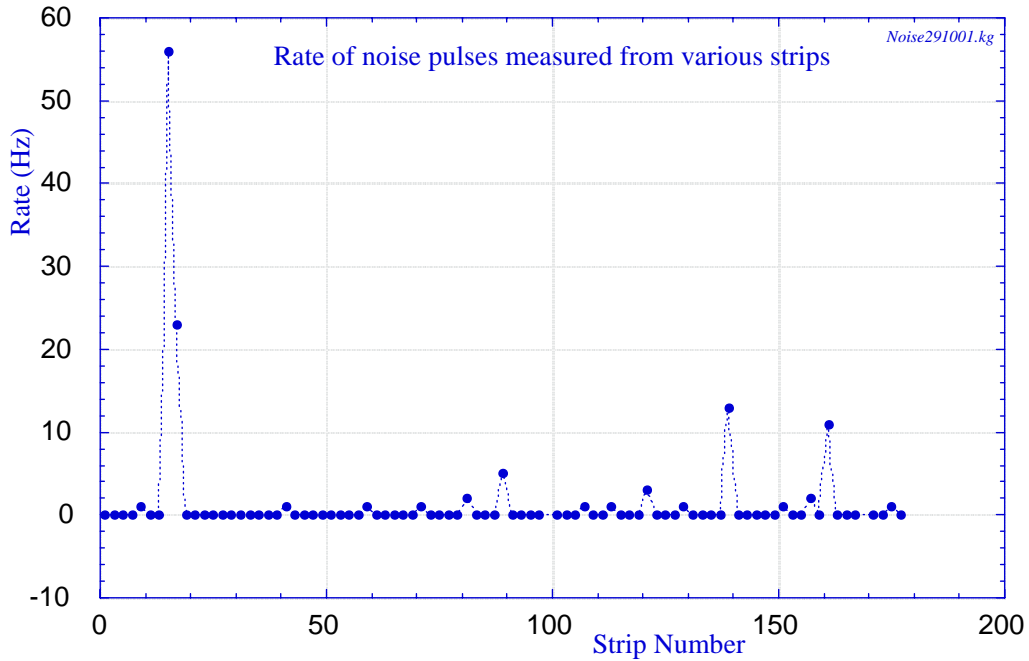


Fig. 15

The main conclusions from our studies can be formulated as follows: it is impossible to completely avoid noise pulses, but one can strongly reduce their rate by an optimization of the gas mixture, by using smooth surface electrodes, and assembling RPCs in dust free rooms. Some noise measurements with parallel-plate chambers made of metallic electrodes (see Section II) were performed. The results showed that they had no noise at all, suggesting that the noise pulses are associated with the resistivity of the electrodes.

III-2. Supression of Sparks and Glow Discharges

As was shown in our previous studies, maximum achievable gain in parallel-plate chambers with metallic electrodes drops with rate due to discharges [17]. It was found that the same is true for RPCs with low resistivity electrodes ($<10^4 \Omega\text{cm}$) An example of a spark type of breakdown at high rates is shown in Fig 16(a and b). However, in the resistivity range 10^4 - $10^8 \Omega\text{.cm}$ a new phenomenon has been observed: a glow discharge Fig 16 (c and d). Contrary to the sparks, the duration of this discharge can be very long from a fraction of μs up to infinity. From the point of view of damage to the electronics, this type of discharge is more dangerous compared to sparks. This is simply because in RPCs the energy of a spark is limited, a glow discharge delivers a lot of energy and therefore easily destroy electronics. Surprisingly, in some range of the electrode resistivities the glow discharge appears even at low rates. To identify the resistivity regions at which spark or glow discharge occur, we performed studies with a wide range of resistivities of electrodes. The results of our measurements are summarized in Fig 17.



Fig. 16 Spark left(a) right(b)

Scale: a) For both signals 50 ns, 5mV

b)Top 50 ns, 0.5V, Bottom 50 ns, 100 mV

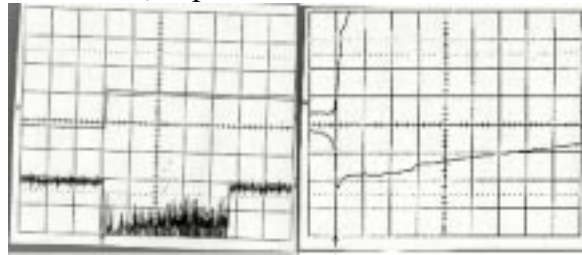


Fig. 16 Glow-Discharge left (c) right (d)

Scale: c) For both signals 50 μ s, 5V

d)Top 0.1 μ s, 5V, Bottom 0.1 μ s,100 mV

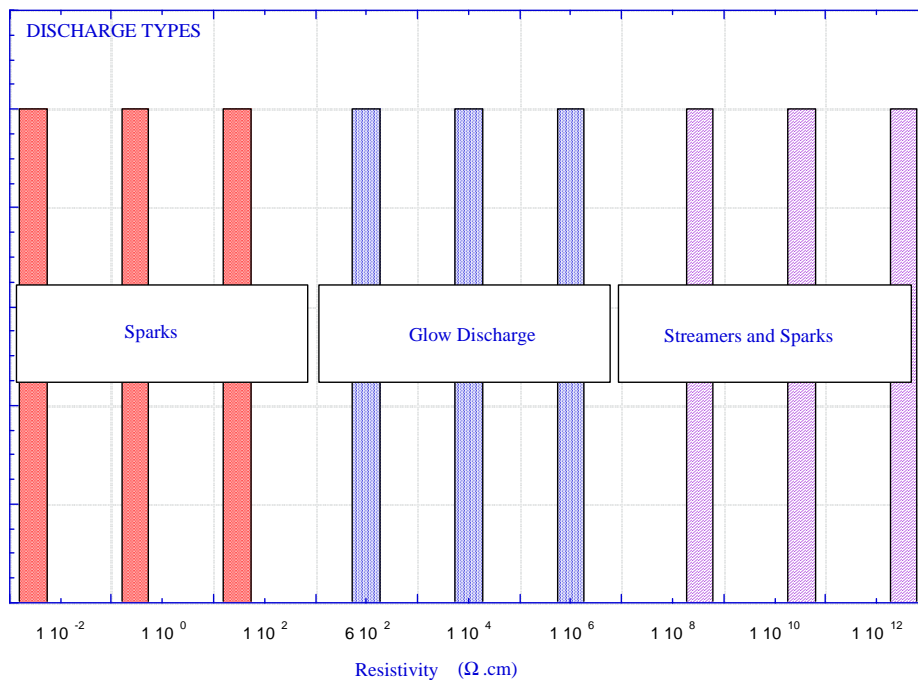


Fig. 17

One observes that at low and high resistivities a spark type of discharge dominates, while in a “medium” range of resistivities (10^4 - $10^8 \Omega \cdot \text{cm}$), the glow type discharge dominates. Detailed studies have been performed to find the conditions for the glow discharge suppression with the conclusion that it is almost impossible fully suppress it. However it was possible strongly reduce the duration of the glow discharge (up to

a fraction μs) by using highly quenching mixtures, for example high (<25%) concentration of ethane in Ar-ethane based mixtures. Note that in the spark region highly quenching mixtures do not have any effect. Partial suppression of the glow discharge by using highly quenched mixtures may lead to other serious problems of aging and surface coating by absorbed layers. Aging creates “weak” points on the RPC cathodes (depositions) and we observed in the simulation studies an enhancement of electric field at the edges of imperfections/depositions. The absorbed layer leads to bursts of noise pulses, most likely due to the Malter effect. The best preliminary results from the point of view of suppression of the glow discharge, without bursts of noise pulses were obtained in operational mixtures of Argon with freon, alcohol vapors. However no long term tests were performed.

III-3 Micro-RPC with secondary electron emitters

- Optimization of the secondary electron emitters

RPC with porous CsI secondary electron emitters have been described elsewhere [18]. The main advantage of this approach is that it allows to improve the time resolution of the RPCs, as well as its efficiency. However, porous CsI emitters are easily charged up and therefore can be used only at low rates, $<10^3\text{Hz/cm}^2$.

Note that porous CsI emitters have advantages only for the detection of the minimum ionizing particles. For the detection of X-rays one can use thin ($0.4\mu\text{m}$ thick) uniform CsI layers. If X-rays enter the CsI emitter at a shallow angle, it has enough probability for absorption, and at the same time, secondary electrons created after the X-ray absorption can be easily be emitted [19]. Below we describe our results for this kind of approach.

- Position resolution optimization: The micro-RPC

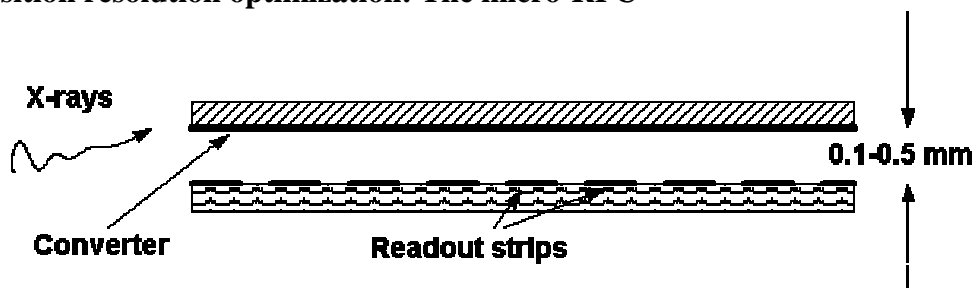


Fig. 18

The position resolution limit in micropattern detectors is determined by the length of the region available to electrons to be converted by radiation in the gas (primary electrons). In addition, diffusion in the drift and the geometry of the amplification region play a vital role. Obviously, in order to achieve the best possible position resolution one has to optimize each of these parameters. The minimum possible length available for primary electrons can be achieved by using solid converters of radiation. In this case, primary electrons are created mostly inside a thin solid layer and some (sometimes all) of primary electrons could be extracted (by applying a strong electric field across it) into the gas media and then multiplied. A minimum spread due to diffusion one can achieve by using a minimum possible gap between the converter and the amplification region. A minimum avalanche size can be ensured

by using a small multiplication region. This leads to a concept of a micropattern detector with a solid converter immediately (without any drift region) followed by an immediate amplification region without any drift space, the micro-RPC. One possible design of a such detector is shown in Fig. 29.

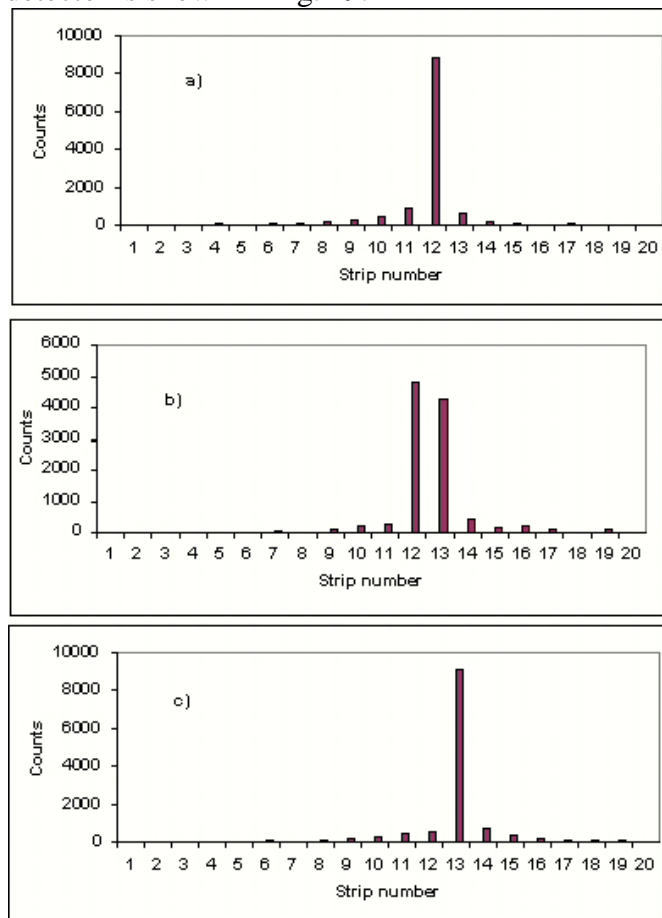


Fig. 19

Fig. 19 a shows an image of a slit $30\ \mu\text{m}$ wide, placed in front of the detector (0.4 mm gap) perpendicular to the anode strips and to the electrodes plates. Figures 19 (b,c) show the images of the same slit shifted each time by 15 micron in a direction perpendicular to the strips. During further movement of the slit this movement is periodically repeated. In fig. 19, for simplicity, only one period is presented. From an image contrast (ratio of counts from neighboring strips) one can conclude that a position resolution better than 30 micron was achieved. Note that due to the feature of a parallel plate structure in which the maximum multiplication obtained electrons created near the cathode, almost the same position resolution could be achieved without a converter, however the efficiency was very low.

IV. Discussion:

As mentioned in the introduction, at high rates ordinary (high resistivity) RPC suffers from several problems: charging up of their electrodes, current and spurious noise pulses. The charging up effect can be diminished by using low resistivity materials for the electrodes; it was found that even low resistivity materials ($\sim 2000\ \Omega\cdot\text{cm}$) are able to efficiently protect electronics. We demonstrated that some part of the leakage current is associated with the noise pulses while the other with a leakage current

occurring through spaces and supporting frames. By a proper shaping of spacers and frames edges the latter component of leakage current can be minimized, however at the same time one has to reduce the resistivity of electrodes to ensure good RPC performance, hence a good compromise can be found. Concerning the noise pulses we remind that in a parallel-plate chamber with metallic electrodes they are practically absent suggesting that they are associated with the electrode resistivity. Based on our earlier studies [17] we may speculate that the origin is a Malter-type effect: the positive ions deposited on the cathode surface create high local electric field, and this causes an emission of electron jets containing several primary electrons. This is why noise pulses appear at voltages when RPCs becomes sensitive to single electrons (its efficiency close to 100%). One also can speculate that the loss of the efficiency of high resistivity RPCs with an increase in voltage is also associated with these noise pulses.

We found that current due to the noise pulses could be minimized by using low resistivity electrodes. It is also very important to use electrodes with well-cleaned smooth surfaces. All dust particles should be removed by ultrasonic cleaning in distilled soap water. RPC assembly should be done in a dust free clean room. One should also avoid, when using gases with vapors, creating an adsorbed layer and also gases which “age” (produce polymer films on the RPCs) cathodes. As a result of all these efforts the counting rate due to the noise pulses could be strongly diminished. Efficiency of these RPC’s in detecting minimum ionizing particles only slightly decreases with voltage in contrast to the high resistivity RPC’s.

The other important achievement in this work was a demonstration of an extremely good position resolution (better than 50 μ m) of a small gap micro-RPC. This high position accuracy was obtained in a simple counting mode, without using any treatment method (like center of gravity). This immediately affords the use of small gap micro-RPC’s for digital imaging and may be further optimized by an increase of pressure.

V. Conclusions and Outlook

Detailed studies of the origin of noise in standard RPCs have been investigated, materials, geometry and operating conditions have been optimized. We have demonstrated that a small gap micro-RPC made of low resistivity materials combines high rate capability, approaching that of metallic parallel-plate chambers, with extremely good position resolution and electronics protection features. We believe that with further studies and optimizations these type of RPCs may find a wide range applications for example in medical imaging, biology, crystallography and as a high rate capable tracking device.

Acknowledgments

The authors would like to thank G. Aielli, S. Biagi, W. Riegler, W. Vandoninck and R. Veenhof and for their valuable discussions and contributions to this work. We are grateful to C. Gustavino and G Manoki for supplying us with some glass RPCs.

References:

- [1] I. Crotty, P. Fonte, D. Lemenovski, V. Peskov “A new resistive plate chamber with secondary electron emitters and two-dimensional microstrip readout” Proceedings of the IEEE Nucl.Sci Sympos (Conf. Record), Anaheim, CA 1996 v1, pp362-366
- [2] P. Fonte, N. Carolino, Y. Ivaniochenkov, V. Peskov “A new material for extremely high counting rate proportional mode RPCs. Proceedings of IV International Workshop on resistive plate chambers and related detectors ; Napoli 1997; Scientifica Acta v. XIII,#2 p11 (1998)
- [3] E. Ceron-Zeballos, I. Crotty, P. Fonte, D. Hatzifotiadou, J. Iamas Valverde, V. Peskov et al., ”New developments on RPC: secondary electron emission and microstrip readout” Proceedings of III International Workshop on resistive plate chambers and related detectors ; Pavia 1995; Scientifica Acta v. XI,#1, p45-61 (1996)
- [4] E. Ceron-Zeballos, I. Crotty, D. Hatzifotiadou, J. Iamas Valverde, M.C. Williams, A. Zichichi et al., Resistive plate chambers with secondary electron emitters and microstrip readout” Nuclear Instruments and methods in phys Res A392 (1997) 150
- [5] P. Fonte, V. Peskov “Micro-gap parallel-plate chambers with porous secondary electron emitters” Nuclear Instruments and methods in phys Res A392 (2000) 260-266
- [6] C. Gustavino, M D’Incecco, E. Tatanni, G. Trincherò “A glass resistive plate chamber for large experiments” Nuclear Instruments and methods in phys Res. A457 (2001)558-563
- [7]. Peskov, C. Gustavino, G-P. Manikki “Some studies of the MONOLITH RPC’s” MONOLITH internal report, Sept 2001, Stockholm
- [8] V. Peskov, B.D. Ramsey, P. Fonte “Surface streamer breakdown mechanisms in microstrip gas counters” Nuclear Instruments and methods in phys Res A454 (1997) 89-93
- [9] V. Korablev et al, "*Electric field and currents in resistive plate chamber*", IHEP Preprint 96-52, Protvino 1996
- [10]. R. Santonico see for example, Proceedings of the several RPC conferences.
- [11] CMS (Korean) Measurements Private Communication, September 2001
- [12] E. Gorini et al, "*Measurement of drift velocity and amplification coefficient in C₂H₂F₄-isobutane mixtures for avalanche-operated resistive-plate counters*", Nucl. Instr. and Meth. A 425 (1999) 84-91
- [13] S. F. Biagi, private communication
- [14] P. Cwetanski, A. Romaniouk, V. Sosnovtsev, "*Studies of wire offset effects on gas gain in the ATLAS TRT straw chamber*", ATLAS Internal Note ATL-INDET-2000-16
- [15] G. Aielli, "*Advanced studies on RPCs*", Doctorate Thesis, December 2000, Univ. Roma “Tor Vergata”; W. Riegler, private communication to be published, Oct. 2001
- [16] P. Fonte, A. Smirnitski, M.C. Williams, “A new high-resolution TOF technology” ; Nucl. Instrum. Methods Phys. Res., A : 443 (2000) no.1, pp.201-4
- [17] P.Fonte, V. peskov, B. ramsey “The fundamental limitations of high-rate gaseous detectors”IEEE Trans. Nucl Sci,v.46pp312-315,1999
- [18] P. Fonte, V. Peskov, “ Gain, Rate and Position Resolution Limits of Micropattern Gaseous Detectors” Preprint LIP-2001-06. - 5 Jun 2001. - 10 p. (physics/0106017)
- [19] A. Breskin “Secondary emission gaseous detectors : a new class of radiation imaging devices” Nucl. PhysB44(1995) 351-363.